

# Journal of Biomedical Optics

[SPIEDigitalLibrary.org/jbo](http://SPIEDigitalLibrary.org/jbo)

## ***In vivo* detection of inhalation injury in large airway using three- dimensional long-range swept-source optical coherence tomography**

Lidek Chou  
Andriy Batchinsky  
Slava Belenkiy  
Joseph Jing  
Tirunelveli Ramalingam  
Matthew Brenner  
Zhongping Chen

# *In vivo* detection of inhalation injury in large airway using three-dimensional long-range swept-source optical coherence tomography

Lidek Chou,<sup>a,b</sup> Andriy Batchinsky,<sup>c</sup> Slava Belenkiy,<sup>c</sup> Joseph Jing,<sup>a,d</sup> Tirunelveli Ramalingam,<sup>b</sup> Matthew Brenner,<sup>a,e</sup> and Zhongping Chen<sup>a,d,\*</sup>

<sup>a</sup>University of California, Beckman Laser Institute, 1002 Health Sciences Road East, Irvine, California 92612

<sup>b</sup>OCT Medical Imaging Inc., 1002 Health Sciences Road East, Irvine, California 92612

<sup>c</sup>US Army Institute of Surgical Research, San Antonio Military Medical Center, Fort Sam Houston, San Antonio, Texas 78234

<sup>d</sup>University of California, Department of Biomedical Engineering, Irvine, California 92697

<sup>e</sup>University of California, Irvine Medical Center, Division of Pulmonary and Critical Care, Orange, California 92868

**Abstract.** We report on the feasibility of using long-range swept-source optical coherence tomography (OCT) to detect airway changes following smoke inhalation in a sheep model. The long-range OCT system (with axial imaging range of 25 mm) and probe are capable of rapidly obtaining a series of high-resolution full cross-sectional images and three-dimensional reconstructions covering 20-cm length of tracheal and bronchial airways with airway diameter up to 25 mm, regardless of the position of the probe within the airway lumen. Measurements of airway thickness were performed at baseline and postinjury to show mucosal thickness changes following smoke inhalation. © 2014 Society of Photo-Optical Instrumentation Engineers (SPIE) [DOI: [10.1117/1.JBO.19.3.036018](https://doi.org/10.1117/1.JBO.19.3.036018)]

Keywords: optical coherence tomography; long-range optical coherence tomography; smoke inhalation injury.

Paper 130820RR received Nov. 18, 2013; revised manuscript received Feb. 25, 2014; accepted for publication Feb. 28, 2014; published online Mar. 24, 2014.

## 1 Introduction

The diagnosis of inhalation injury is a primary unresolved problem in modern burn care.<sup>1</sup> Up to 20% of patients admitted to burn centers suffer from smoke inhalation injury, which frequently leads to respiratory failure, mechanical ventilation, and increases the predicted mortality by 20% to 60% over risk associated with burn alone.<sup>2</sup> Pathophysiological changes begin in the airway upon initial smoke exposure but generally go undetected due to a lack of sensitive diagnostic capabilities.<sup>3–5</sup> Optical coherence tomography (OCT) is a high-resolution imaging modality that is capable of providing images at near histopathological resolution. The OCT can be used to image tissue structures with a penetration depth of ~2 to 3 mm, allowing visualization of the mucosa and submucosa of airways. Previous studies have reported *in vivo* detection of smoke-induced airway injury and quantification of airway thickness changes with three-dimensional (3-D) OCT imaging on rabbits.<sup>6,7</sup> However, large-airway structures such as the human trachea have internal diameters exceeding the typical OCT axial imaging range or imaging depth of 5 mm; therefore, an OCT system with an extended imaging range is necessary to image the full circumference of the larger diameter human airways including the trachea and mainstem bronchi. The development of anatomic long-range OCT (LROCT) has been described for studying the full circumference of airway lumens, but previous reports used mechanically actuated reference delay arms that limit image acquisition speeds.<sup>8,9</sup> Our group has previously developed a LROCT system utilizing an acousto-optic modulator (AOM) that allows for rapid, real-time, dynamic monitoring, and large 3-D volume imaging over the entire upper airway with an axial imaging range up to

15 mm in depth.<sup>10</sup> Based on the previously reported long-range system, we have further improved and developed an OCT system prototype for clinical use. The improved system completes a 20-cm-longitudinal scan of airway in 16 s, and has an extended imaging range of 25 mm. This range is sufficient to cover a normal human lower airway regardless of where the OCT imaging probe is positioned within the lumen, whereas the upper limits for coronal and sagittal diameters of tracheal air column are 25 and 27 mm in men and 21 and 23 mm in women, respectively.<sup>11</sup> We have evaluated this new system in a sheep model which was exposed to wood-bark smoke inhalation injury and 40% total body surface area full thickness burn. Our goal was to use LROCT to achieve real-time near histology grade evaluation of airways that could be useful for rapid non-invasive assessment of inhalation injury.

## 2 Materials and Methods

### 2.1 OCT System and Probe

The improved LROCT system prototype (shown in Fig. 1) was designed for imaging human subject airways in a clinical setting. The OCT interferometry unit incorporates the same overall design as our previously reported setup, utilizing a 1310-nm swept laser source (50 kHz A-line scan rate, 29.4-mW average power, and 109-nm bandwidth at 10 dB, Axsun Technologies, Billerica, Massachusetts) and an AOM (Brimrose Corp., Sparks, Massachusetts) to generate a carrier frequency for the OCT signal; the main difference lies in the AOM in which the current setup generates a frequency shift of 150 MHz as opposed to 100 MHz in our previous setup.<sup>10</sup> The higher carrier frequency allows further utilization of the swept laser source coherence

\*Address all correspondence to: Zhongping Chen, E-mail: [z2chen@uci.edu](mailto:z2chen@uci.edu)



**Fig. 1** Long-range optical coherence tomography (LROCT) system clinical prototype. The main OCT system contains all the major optical and electrical components necessary for LROCT imaging, as well as supplying the necessary power for the imaging probe control unit, which is responsible for OCT imaging probe rotation and pull back. The computer unit with a commercial graphics processing unit rapidly acquires and processes the OCT data and provides real-time display of two-dimensional (2-D) cross sections of airway. Three-dimensional (3-D) reconstructions are then performed using the acquired 2-D images with the help of a commercial software.

length achieving  $\sim 25$ -mm axial imaging range. Data acquisition is achieved through the use of a 1-GHz digitizer (Alazar Technologies Inc., Pointe-Claire, Quebec) to accommodate the wider OCT signal bandwidth resulted from the 150-MHz frequency shift. Imaging of airways with a maximum diameter of 50 mm can be achieved with this system if the OCT probe can be positioned in the center of an airway lumen. The imaging probe control unit in Fig. 1 proximally rotates the entire probe at 1500 rpm to achieve 25 frames/s (2000 A-lines per frame) with a pull back speed of 12.5 mm/s to minimize the time for full airway length imaging for assessment of clinical conditions such as inhalation injury diagnosis. Due to the high speed acquisition of LROCT data, the computer system is equipped with a commercial graphics-processing unit (GPU) for displaying real-time two-dimensional (2-D) cross sections. In order to achieve a high-rotation speed, the OCT probe, with schematic shown in Fig. 2(b), is constructed using a stainless torque coil [0.965-mm outer diameter (OD), Asahi Intecc, Santa Ana, California] for translating torque from the proximal end of the probe to the distal end of the probe. From the most proximal portion of the probe tip, a single-mode fiber is fused to a portion of no core fiber whose length determines the working distance of the probe. In front of the no core fiber portion an angle cut gradient index lens with a 1-mm OD is used to focus the diverging laser beam onto a 45-deg gold-coated rod mirror. The incident light on the mirror is then reflected at 45 deg relative to the incident beam creating a side-viewing probe. The optical assembly at the probe tip is protected by a metal housing that is firmly soldered to the torque coil by inserting  $\sim 2$  mm of coil inside the metal housing and

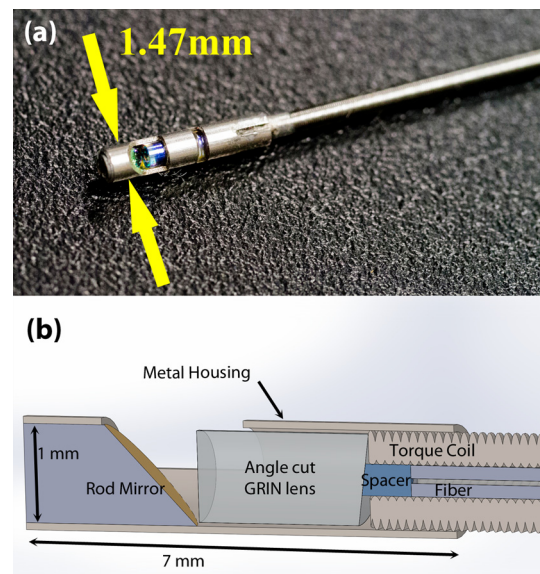


**Fig. 2** (a) A photograph of and (b) the schematic of OCT imaging probe tip. This probe features an angle cut gradient index (GRIN) lens and a rod mirror both 1 mm in diameter, secured in a 7-mm-long stainless steel metal housing that is soldered to the stainless torque coil for protection of the optical components. A single mode SMF-28 fiber inside the torque coil is used to carry the laser beam and the length of spacer determines the working distance of the probe. The maximum diameter of the imaging probe is 1.47 mm.

applying a small amount of lead-free solder to the junction between the housing and the coil, allowing the solder to seep in and fill the gap between the two components to increase the robustness of the entire probe assembly as shown in Fig. 2(a). As previously reported, in order to achieve long-range imaging, the probe was designed to have an extended working distance of 20 mm and the axial resolution of the system was  $10 \mu\text{m}$  in tissue.<sup>10</sup> However, even though the system is capable of achieving imaging range of up to 25 mm, the working distance of the probe is usually chosen to closer match the estimated dimension of an airway lumen instead of optimizing for maximum imaging range of the system.

## 2.2 Animal Preparation

The experimental protocol was approved by the U.S. Army Institute of Surgical Research Institutional Animal Care and Use Committee and the UC Irvine IACUC. The study has been conducted in compliance with the Animal Welfare Act; the Implementing Animal Welfare Regulations and in accordance with the principles of the Guide for the Care and Use of Laboratory Animals. The system was tested on a convenience sample from an ongoing study which involves a clinically relevant model of lung failure due to inhalation of wood bark smoke and cutaneous burn.<sup>12,13</sup> After induction of anesthesia an animal was instrumented, which involved percutaneous cannulation of bilateral external jugular veins and left carotid artery under ultrasound guidance as well as tracheostomy. Subsequently, the subject was transferred to a smoke room, where smoke inhalation injury described previously was induced.<sup>13</sup> Postinjury the animal was returned to the ICU, where it was continuously monitored in an intensive care environment for 96 h and was subjected to OCT at multiple time points before and after injury.

### 2.3 OCT Imaging Procedure

As part of the main study fiber optic bronchoscopy was performed using an Olympus Evis Exera II, BF Type Q180 pediatric video bronchoscope (Olympus America, Inc., Center Valley, Pennsylvania). The bronchoscope was first inserted through the tracheostomy tube into the sheep airway by a physician and advanced into the right mainstem bronchus. Under visual control via the bronchoscope the OCT probe with fluorinated ethylene propylene sheath together were advanced into the airway until the probe reached the bronchoscope tip. Next, the bronchoscope was retracted to provide an unobstructed airway field for the OCT probe during imaging. Helical airway cross sections were then acquired by simultaneously mechanically rotating and pulling back the rotating OCT probe over 20-cm length of airway. Because imaging of the trachea and major airways was achieved as an adjunct to routine fiber optic bronchoscopy, the entire (bronchoscopy + OCT) procedure was done with trivial procedure lengths (2 to 3 min) and without complicating the bronchoscopic procedure. After the animal subject was anesthetized but prior to transferring to the smoke room, the aforementioned procedure was done and baseline OCT images were acquired to establish a reference for later comparison of mucosal thickness changes due to injury. The same procedure was repeated and OCT image sets were acquired at 1, 24, 48, 72, and 96-h postinjury. Bronchoscopy cleaning of airways was performed postinjury before OCT imaging when necessary. Three-dimensional reconstruction was performed using the 2-D cross-sectional images acquired and mucosal thickness measurements were performed on the 2-D images to monitor the progression of inhalation injury off line.

### 3 Results

The sensitivity roll off with respect to depth for the LROCT system is shown in Fig. 3, demonstrating a 6- and 20-dB sensitivity roll off at a total imaging range of 12.8 and 22.2 mm, respectively. As can be seen from the sensitivity profile, the maximum sensitivity occurs at a depth of  $\sim 9.5$  mm, which is the result of having a 150-MHz carrier frequency. The asymmetric profile in

Fig. 3 suggests that an AOM with a higher frequency shift than the currently employed 150-MHz model may further extend the imaging range, or simply improve the sensitivity roll off for imaging ranges greater than 19.7 mm (symmetrical portion of the roll off profile indicated by light blue background in Fig. 3). Even though the sensitivity continues to roll off with depth, features can still be seen up to 25 mm. For this feasibility study, with the prior knowledge of an estimated airway lumen size, the working distance of the probe was shortened from 20 to 10 mm to give a  $1/e^2$  beam diameter of  $119 \mu\text{m}$  at the focal plane and a Rayleigh range of  $\sim 7.2$  mm, measured using a beam profiler (DATARAY INC., Bella Vista, California). Figure 4 shows an example of a 3-D reconstruction image of sheep airway acquired using the long-range system. The 3-D image was reconstructed from using 400 cross-sectional OCT images acquired in a single pull back of 20 cm at 12.5 mm/s, with 500- $\mu\text{m}$  longitudinal separation between each cross section. From the reconstructed image, branching features can be clearly identified, including the bifurcation at the carina to the left mainstem as well as secondary bronchi (and the branch to right cranial lobe off the right lateral trachea present in sheep). For monitoring the conditions and progression of smoke inhalation injury in the sheep airway, OCT images were acquired from closely coregistered sites, identified by anatomical landmarks at various time points including baseline, post injury at 1, 24, 48, 72, and 96-h time points. Two-dimensional cross sections obtained from the right mainstem bronchus near the proximal secondary bronchus branch, indicated by the white line in Fig. 4, are shown in Fig. 5. The circumferential images (transformed from Cartesian images below) in the top row of Fig. 5 show the airway cross sections at the same location in the airway, and the Cartesian images beneath provide better views of the airway substructures. By zooming to the boxed region shown in the Cartesian images, the magnified regions of interest in the bottom row of Fig. 5 show structural similarities at the same imaging site at different time points, and the most distinct feature that can be seen before and after smoke inhalation injury is the underlying cartilage. During LROCT imaging, cartilage is used as a reference to quantitatively monitor the changes in the

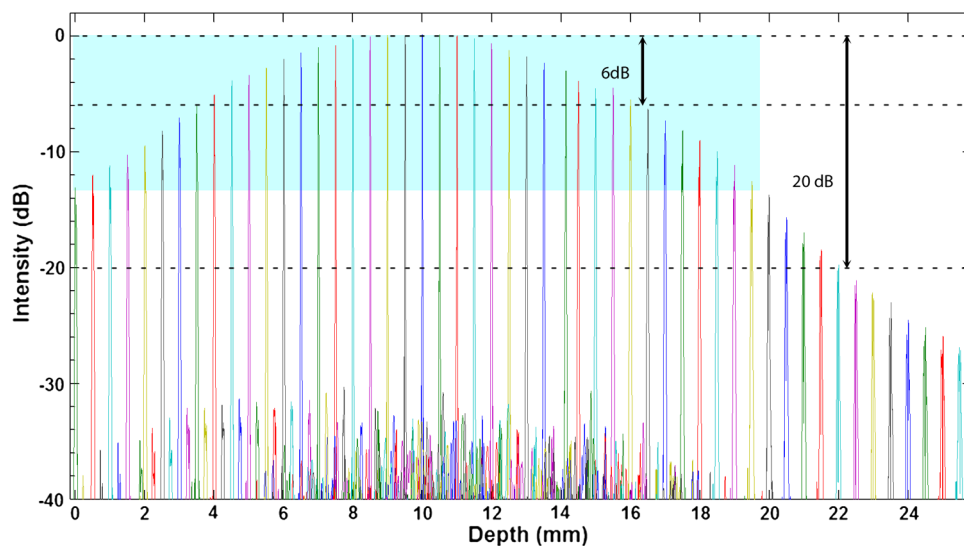


**Fig. 3** Sensitivity of the OCT system with respect to depth. The imaging ranges for 6 and 20 dB sensitivity roll off are 12.8 and 22.2 mm, respectively. For the symmetrical portion of the sensitivity roll off profile, the imaging range is 19.7 mm.

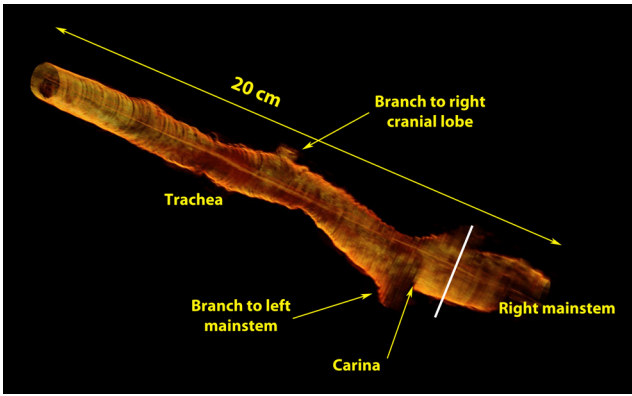


**Fig. 4** Three-dimensional reconstruction image of sheep airway using images acquired by the LROCT system prototype. The reconstructed image shows the sheep airway covering from the trachea down to the beginning segment of right mainstem bronchus (RMB). Branches to the left mainstem bronchus and right upper lobe takeoff (white line), as well as a branch to the right cranial lobe can be clearly seen.

mucosa and submucosa, since the cartilage has distinct boundaries and is relatively homogenous, appearing as a well demarcated anatomical structure.<sup>6,7</sup> From the images in the bottom row of Fig. 5, cartilage can be seen as the underlying dark region in images from all of the time points. Using the boundary between the cartilage and the tissue layers above as a reference, thickness measurements were performed at two sites (same for all time points) located at the entrance to the right upper lobe takeoff indicated by the dotted lines in the bottom row of Fig. 5. Mucosal thickness measurements are then plotted to show

the changes in airway images over time. At baseline, mucosal thicknesses were 0.52 and 0.87 mm at the left and right measurement sites, respectively. Mucosal thickening was seen at the same sites within an hour following smoke inhalation at 0.78 mm (left) and 1.15 mm (right), and continued to increase to 1.77 mm (left) and 1.86 mm (right) 24-h postinjury. The mucosal thickening was most pronounced at 48 h after injury and was measured to be 2.02 mm (left) and 2.16 mm (right), which is about three times the thickness measured at baseline. As would be expected, after bronchoscopic cleaning of the airways and debridement of airway casts and sloughed off epithelium performed as part of the main study protocol at 48 h, thinning of the remaining mucosa at the entrance to the right upper lobe takeoff was observed on the 72-h (left 1.17 mm, right 1.58 mm) and 96-h (left 1.12 mm, right 1.50 mm) post-injury OCT images (Fig. 5). Measurements of mucosal thickness at different time points are plotted in Fig. 6. From the imaging and measurement results provided here it is clear that smoke inhalation caused injury and thickening of the mucosa and submucosa within an hour of, if not immediately after, smoke inhalation. Because bronchoscopy was performed 1 h after the injury we could not assess the changes immediately postexposure to smoke as we simply followed the main study timeline and did not perform a dedicated bronchoscopy for the sake of performing OCT imaging alone.

#### 4 Discussion

Diagnosis of inhalation injury and correlation between bronchoscopic imaging or x-ray computed tomography scan and clinical parameters of lung injury is a critical unmet need recognized by the American Burn Association, which can be fulfilled

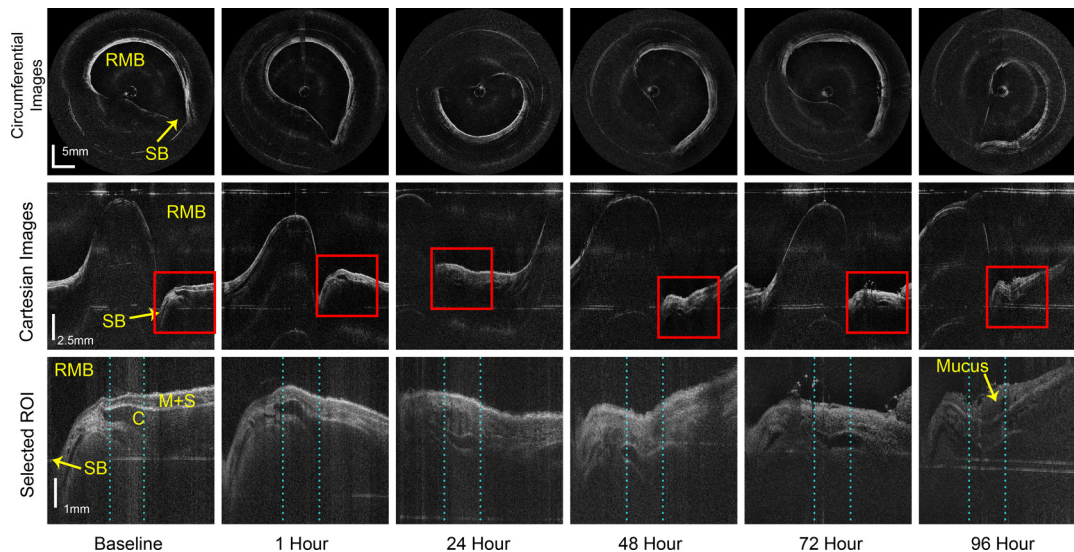


**Fig. 5** OCT images of sheep airway obtained near the proximal secondary bronchus (right upper lobe takeoff) (SB) in the RMB. The 3 × 6 image grid is displayed with each row showing the same view, and each column shows the same time point. Top row: circumferential images showing the contour of the airway lumen, the shape and size of the lumen are nearly identical for all the images, the orientation of the cross sections vary due to different starting position of a scan; The emerging SB branch shows up as a “pointy” region on the contour of airway lumen, which corresponds to a “trench-like” region in the Cartesian images. Middle row: Cartesian images of the same cross section as the circumferential images, for easier examination and measurement of the tissue structure; Bottom row: magnified views of the selected regions of interest shown in red boxes in the corresponding Cartesian images above. Thickness of the mucosa and submucosa (M + S) for all time points were measured using underlying cartilage (C) as a reference. Blue dotted lines represent the two chosen sites for thickness measurements.

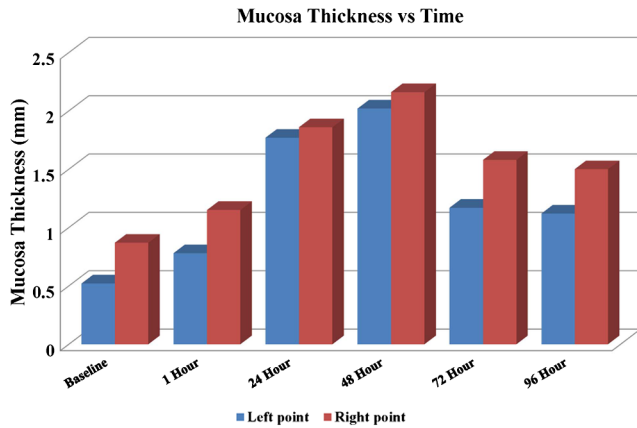


**Fig. 6** Mucosal thickness versus time. Thickening began within 1 h following smoke inhalation, progressed to peak at 48-h postinjury. Left point and right point data correspond to mucosal thickness measured at the positions indicated by the left and right dotted lines shown in Fig. 5, respectively.

via LROCT imaging. Prior studies have demonstrated using OCT for smoke inhalation injury studies on small animal subjects, but those systems were limited to a maximum imaging range of 2.9 mm with 6-dB roll off at 2.2 mm, making them impractical for imaging larger diameter airways such as the human trachea.<sup>6,7</sup> Therefore, we posit that LROCT is useful for both 2-D and 3-D evaluation of larger airway mucosa and obtained similar results in this large-animal feasibility study. From Figs. 5 and 6, we show qualitative and quantitative changes in mucosal thickness similar to the results presented in prior studies.<sup>6,7</sup> However, we cannot yet establish a relationship between the mucosal thickness changes and the real injury, since future studies with larger sample size are required to perform statistical analysis on measurements in order to establish such a relationship. A refined measurement method is also necessary. For example, while all the measurements were acquired at a closely coregistered site in the lower airway, and cartilage rings appeared to be excellent reference points when measuring mucosal thickness, tissue structures imaged at different time points appeared slightly different due to physiological changes in tissue as well as other external factors. Therefore, measurements based on a single cross section might be inaccurate. One possible method is to lower the pull-back speed and perform a short pull back (e.g., a few centimeters) over a longitudinal section of interest, essentially reducing the spacing (currently 500  $\mu\text{m}$ ) between each cross section, and average the measurements from closely spaced, adjacent cross sections to obtain more accurate results. However, while this method can potentially improve the measurement accuracy, it increases the entire procedure length significantly, which potentially has negative influences on the overall wellbeing of a patient. It is possible to increase the rotation speed of the probe to decrease overall scanning time to compensate, but our current probe was not designed to withstand higher rotational speeds, which would cause warping artifacts in images due to nonuniform rotation. For future studies, we plan to further improve the structural integrity of our probes to handle higher rotation speed, consequently increasing the frame rate by lowering the number of A-lines per frame, which is currently set higher than necessary for our probes with relatively large-spot sizes. Further improvements on the OCT system includes the use of an AOM with

higher modulation frequency mentioned in Sec. 3, and upgrading the laser source with one that has inherently longer coherence length to enhance the sensitivity throughout the entire imaging range. Finally, we want to point out that the animals in this study are anesthetized, intubated with subsequent placement of a tracheostomy, and then exposed to smoke in anesthetized state. As such this model is not identical to conscious inhalation of smoke in terms of pulmonary mechanics and lack of cough, sneezing and avoidance of smoke which would be observed in conscious state. This experimental model has been chosen to cause lung injury and the smoke exposure technique *per se* is not pursued for its relevance to conscious inhalation injury because of animal welfare consideration. There may be difference in the smoke uptake between animals in conscious and anesthetized state. Furthermore, the oral and nasal cavity deposition in sheep would be quite different from that seen in humans. Therefore, extending our current animal results to human cases requires further investigation.

## 5 Conclusion

We have demonstrated an improved LROCT system with up to 25-mm imaging range, as well as demonstrated the feasibility of using our LROCT system to qualitatively and quantitatively assess the progression of smoke inhalation injury over time. Compared with the previously reported anatomic LROCT that utilized mechanically actuated delay arms as to achieve scanning distance of 26 to 27 mm, our swept-source LROCT with AOM not only has nearly identical imaging range but can also achieve much higher frame rate of 25 Hz (at 2000 A-lines per frame) as opposed to 5 Hz (at 800 A-lines per frame).<sup>8,9</sup> The LROCT system showed excellent capability for monitoring changes of airway thickening over time and tracked progressive thickening of the airway mucosa as the injury progressed. The OCT-measured airway injury reached a peak at 48-h postinjury when mucosal thickness was three times higher than baseline. At later time points, as would be expected due to repeated bronchoscopically performed airway cleanings, removal of casts, and sloughed epithelium, we observed a reduction in mucosal thickness. This work is significant in demonstrating the capabilities for rapid, repeated, high-resolution airway imaging, and multidirectional 2-D and 3-D reconstruction capabilities in large airways. These capabilities now enable accurate assessment over time, and determination of tissue structure and changes throughout the full surface and subsurface of large-airway regions *in vivo* as shown. Such capabilities are important in inhalation airway injury where assessment of extent of injury, and risk is essential for early intervention decisions. This technology will be applicable to a broad range of diagnostic conditions, for determination of injury severity, progression, and response to therapy.

## Acknowledgments

We would like to thank Dr. Sari Mahon at UC Irvine for her assistance with IACUC approval, logistics of the study preparation. Mr. Max Wiedmann, Mr. Emon Heidari, Dr. Jun Zhang for their assistance with the system development. Dr. Corina Necsoiu, Dr. Stefan Kreyer, Mr. Pete Walker at the U.S. Army Institute of Surgical Research for their assistance during image acquisition. This work is supported by Military Medical Photonics Program AFOSR Grant # FA9550-10-1-0538 to UCI and DoD Award W81XWH-09-C-0023 to OCT Medical Imaging.

## References

1. T. L. Palmieri, "Inhalation Injury Research Priorities and Needs for the Future," <http://www.ameriburn.org/SOS/InhalationInjury.pdf> (30 September 2013).
2. K. Z. Shirani, B. A. Pruitt, Jr., and A. D. Mason, "The influence of inhalation injury and pneumonia on burn mortality," *Ann. Surg.* **205**(1), 82–87 (1987).
3. L. C. Cancio, "Current concepts in the pathophysiology and treatment of inhalation injury," *J. Trauma* **7**(1), 19–35 (2005).
4. G. B. Hubbard et al., "The morphology of smoke inhalation injury in sheep," *J. Trauma* **31**(11), 1477–1486 (1991).
5. B. A. Pruitt, Jr. and W. G. Cioffi, "Diagnosis and treatment of smoke inhalation," *J. Intensive Care Med.* **10**(3), 117–127 (1995).
6. J. Yin et al., "In vivo early detection of smoke-induced airway injury using three-dimensional swept-source optical coherence tomography," *J. Biomed. Opt.* **14**(6), 060503 (2009).
7. M. Brenner et al., "In vivo optical coherence tomography detection of differences in regional large airway smoke inhalation induced injury in a rabbit model," *J. Biomed. Opt.* **13**(3), 034001 (2008).
8. J. Armstrong et al., "In vivo size and shape measurement of the human upper airway using endoscopic long-range optical coherence tomography," *Opt. Express* **11**(15), 1817–1826 (2003).
9. B. Lau et al., "Imaging true 3-D endoscopic anatomy by incorporating magnetic tracking with optical coherence tomography: proof-of-principle for airways," *Opt. Express* **18**(26), 27173–27180 (2010).
10. J. Jing et al., "High-speed upper-airway imaging using full-range optical coherence tomography," *J. Biomed. Opt.* **17**(11), 110507 (2012).
11. E. Breatnach, G. C. Abbott, and R. G. Fraser, "Dimensions of the normal human trachea," *Am. J. Roentgenol.* **142**(5), 903–906 (1984).
12. M. S. Park et al., "Assessment of severity of ovine smoke inhalation injury by analysis of computed tomographic scans," *J. Trauma* **55**(3), 417–427 (2003).
13. I. Batchinsky et al., "Comparison of airway pressure release ventilation to conventional mechanical ventilation in the early management of smoke inhalation injury in swine," *Crit. Care Med.* **39**(10), 2314–2321 (2011).

**Zhongping Chen** is a professor of biomedical engineering and the director of F-OCT Laboratory at University of California, Irvine. He is a co-founder and the board chairman of OCT Medical Imaging Inc. His research group has pioneered the development of Doppler optical coherence tomography. He has published more than 200 peer-reviewed papers. He is a fellow of the American Institute of Medical and Biological Engineering, a fellow of SPIE, and OSA.

Biographies of the other authors are not available.